Scientific Research Publishing

World Journal of Nano Science and Engineering, 2026, 16(4), 205-233
https://www.scirp.org/journal/wjnse
ISSN Online: 2161-4962
ISSN Print: 2161-4954

Analysis and Modeling of Noise in Urban Areas of Cities in Western Ivory Coast by Processing Acoustic Signal

Toa Bi Guié[1], Vangah Wognin[2], Anicet Kouakou[3], Bernard N'Zebaud[1], Sié Ouattara[4], Alain Clement[5]

[1]UFR Sciences and Technologies, University of Man, Man, Côte d'Ivoire
[2]Digital Research and Expertise Unit (UREN), Virtual University of Côte d'Ivoire (UVCI), Abidjan, Côte d'Ivoire
[3]Laboratory of Fundamental and Applied Physics (LPFA), UFR of Fundamental and Applied Sciences, Nangui Abrogoua University, Abidjan, Côte d'Ivoire
[4]Houphouët Boigny National Polytechnic Institute (INPHB), Yamoussoukro, Côte d'Ivoire
[5]LARIS, SFR MATHSTIC, University of Angers, Angers, France
Email: Theodore.toa@univ-man.edu.ci

How to cite this paper: Guié, T.B., Wognin, V., Kouakou, A., N'Zebaud, B., Ouattara, S. and Clement, A. (2026) Analysis and Modeling of Noise in Urban Areas of Cities in Western Ivory Coast by Processing Acoustic Signal. *World Journal of Nano Science and Engineering*, **16**, 205-233.
https://doi.org/10.4236/wjnse.2026.164009

Received: July 7, 2026
Accepted: September 21, 2026
Published: November 2, 2026

Copyright © 2026 by author(s) and Scientific Research Publishing Inc.
This work is licensed under the Creative Commons Attribution International License (CC BY 4.0).
http://creativecommons.org/licenses/by/4.0/

Open Access

Abstract

This thesis analyzes and models urban noise in five neighborhoods of the city of Man: Sari, Capen, Commerce, Dioulaboubou, and Domoraud. Acoustic recordings were made using a Samsung Galaxy A13 smartphone at three time slots (9 a.m., 12 p.m., and 5 p.m.) on three different types of days, then processed using MATLAB with a digital chain reproducing a Class 2 sound level meter. This chain made it possible to calculate acoustic (LAeq, L10, L50, L90, LNP, TNI), psychoacoustic (loudness), and spectral (spectral centroid, energy distribution by frequency bands) indicators, organized around three complementary models: temporal description, nuisance index, and spectral. The results reveal widespread acoustic saturation throughout the urban fabric. LAeq levels range from 66.95 dB(A) in Domoraud to 72.70 dB(A) in the Commerce district, exceeding the daytime threshold of 55 dB(A) recommended by the WHO and Ivorian decree no. 2016-791 by 12 to 18 dB(A). Spectral analysis confirms the predominance of motorized traffic as the main source, with mid-frequencies (200 - 2000 Hz) representing between 43.9% and 79.2% of the total acoustic energy. Each district exhibits a temporal profile consistent with its functional purpose. In light of this situation, the report recommends regulating audible warning devices, creating moderate traffic zones, and integrating acoustic requirements into urban planning documents.

Keywords

Urban Noise, Acoustic Signal, Man, LAeq, MATLAB, Noise Pollution

1. Introduction

The 21st century is marked by rapid and often uncontrolled urbanization, particularly in developing countries. This growth generates, among other nuisances, increasingly concerning noise pollution. Long neglected, it is now recognized by the World Health Organization (WHO) as one of the most threatening environmental factors for human health [1]. Its effects are well documented: chronic stress, sleep disorders, high blood pressure, cognitive deficits in children, and irreversible hearing loss [2] [3]. In Europe, it is estimated that approximately 16,600 premature deaths per year are linked to it [4].

In Africa, this phenomenon takes on a particular dimension. The massive development of motorized two-wheelers, the proliferation of generators, heavy traffic, and informal commercial activities create highly aggressive noise environments [5]. In Côte d'Ivoire, while Abidjan has begun to be documented with 3,018 noise complaints recorded between 2011 and 2022, representing 60% of environmental complaints [6], secondary cities remain largely ignored by acoustic research. The thesis [7] on Abidjan confirms this glaring scientific gap.

The city of Man, capital of the Tonkpi region in western Mali, perfectly illustrates this reality. A rapidly expanding commercial and administrative hub, it concentrates a diversity of noise sources markets, roads, craft activities, places of worship-within a space framed by mountainous terrain that can amplify acoustic reverberation [8]. Yet, no study has ever measured, analyzed, or modeled its urban noise, depriving the authorities of any scientific basis for action.

This absence raises the following central question:

"To what extent does acoustic signal processing allow for the analysis and modeling of urban noise in the Man area, in order to objectively assess the noise exposure levels of the population, identify dominant noise sources, and propose recommendations adapted to the local context?"

This study aims, in general, to analyze and model urban noise in five districts of the city of Man by digital processing of the acoustic signal, in order to assess the levels of noise exposure of the populations and to formulate recommendations for local authorities, in accordance with the recommendations of the WHO and [9]. To achieve this, specific objectives were defined, namely to measure and quantify noise levels in five representative neighborhoods of Man (Sari, Capen, Commerce, Dioulaboubou and Domoraud) at the time slots of 9 AM, 12 PM and 5 PM, over three consecutive days, using audio recordings processed under MATLAB according to a chain reproducing that of a standardized Class 2 sound level meter. We will analyze the spectral and temporal composition of the noise recorded in each neighborhood, through the calculation of L_{Aeq}, the L_{10}, L_{50} and L_{90} percentiles, LCpeak, psychoacoustic loudness (Sones and Phons), the energy distribution by frequency bands and the spectral centroid, in order to establish the acoustic signature of each environment. We compare the measured levels and calculated nuisance indices (L_{NP} and TNI) with WHO recommendations and the standards of the Ivorian decree, in order to formulate concrete recommendations to the deci-

sion-makers of the city of Man.

This study is structured in three chapters. Chapter I: This section presents the theoretical framework, foundations of environmental acoustics, standardized acoustic indicators, health effects of noise pollution, state of the art of studies conducted in sub-Saharan Africa and Côte d'Ivoire, and methods for processing acoustic signals. Chapter II describes the materials and methods: the capture device, the study area with the five districts investigated, the recording protocol at the three time slots, and the digital processing chain developed under MATLAB including filtering, frequency weightings, calculation of acoustic indicators and the three modeling models (temporal, nuisance and spectral).

Chapter III presents the results and their discussion: for each district and each time slot, the calculated acoustic, statistical and psychoacoustic descriptors, followed by the three models developed, a comparative inter-site analysis and a comparison with WHO standards and Ivorian regulations, leading to concrete recommendations.

It concludes with a general summary of the main results and opens up perspectives for future research.

1.1. Nature and Physical Quantities of the Acoustic Signal

Environmental acoustics is defined as the study of the emission, propagation and reception of sound signals in outdoor space [10]. It is particularly interested in the interactions between noise sources and the complex environment of the city, marked by physical phenomena such as reflection, absorption and diffraction.

Sound is a mechanical disturbance propagating in an elastic medium in the form of longitudinal waves (**Figure 1**) [11].

This wave results from a variation in atmospheric pressure around an equilibrium state.

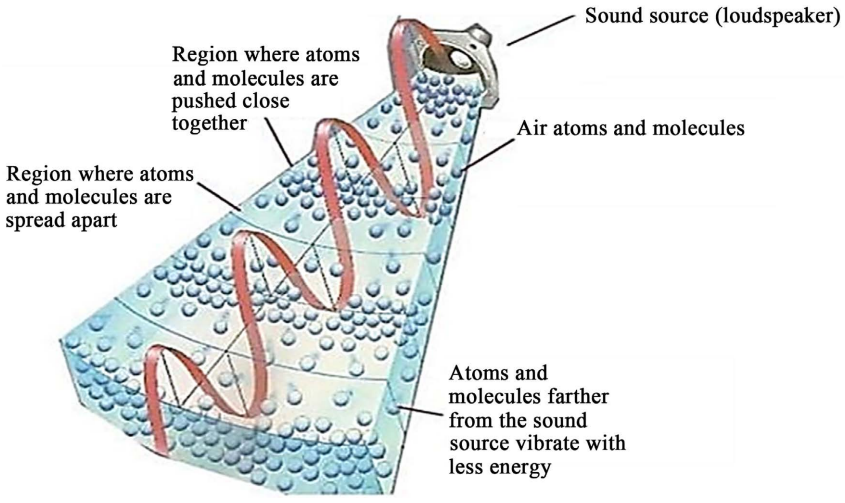


Figure 1. Mechanism of sound wave propagation [12].

Thanks to hearing, we are able to distinguish the pitch of a sound, its loudness,

as well as its position and origin. This perception is based on various physical properties such as frequency, power, intensity and sound level (L) [13].

Sound is a physical phenomenon that produces a sensation of hearing, resulting from a rapid variation in the pressure of air or other elastic media. According to [14] [15], the frequency in Hertz (Hz) defines the number of these variations per second (*i.e.*, the number of periodic oscillations). Depending on the frequency range, sound waves can be classified into three types:

- Infrasound: $f < 20$ Hz;
- Audible sounds: 20 Hz < $f < 20$ KHz, perceptible by humans;
- Ultrasound: $f > 20$ kHz [16] [17].

Furthermore, sounds perceptible to humans are classified according to their frequency into three pitches: low, medium, and high.

Sound power is, according to [18] [19], the amount of energy emitted by a sound source in a unit of time expressed in (W).

Sound intensity, on the other hand, has been defined by [20] as the amount of energy that passes through a surface of one square meter (1 m^2) in one second (**Figure 4**). It is expressed in (w/m^2).

1.1.1. Sound Level (L)

Sound pressure level is a sound characteristic related to the concept of perceived loudness. This parameter depends on the amplitude (**Figure 2**) expressed in dB, given by formula 1.

$$L = 10 \times \log_{10}\left(p^2 / p_0^2\right) \tag{1}$$

where p is the measured acoustic pressure and $p_0 = 20$ μPa is the reference pressure corresponding to the threshold of human audibility.

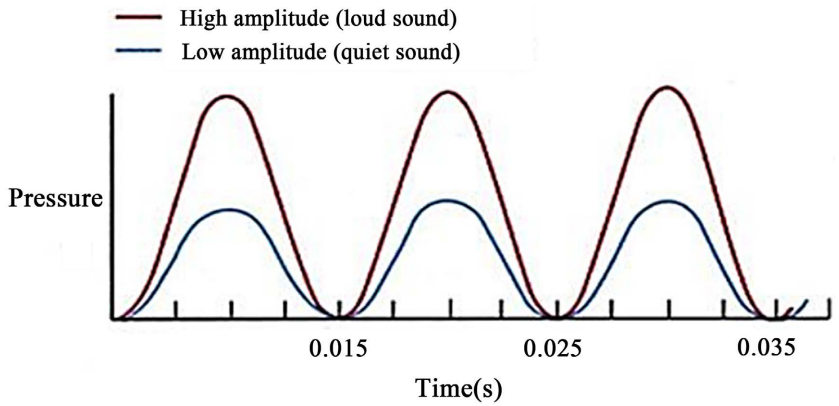


Figure 2. Sound amplitude.

Noise is distinguished from sound by its undesirable nature [21]. In urban acoustics, a distinction is made between: ambient noise (all surrounding noises), background noise (parasitic signals over a given period), and residual noise (sound level in the absence of a specific source). Regulations set thresholds based on emergence, defined as the difference between ambient noise and residual noise

[22]. Since the sensitivity of the human ear is not linear across the entire frequency spectrum, A-weighting, denoted dB(A), is used, which applies a corrective filter simulating the response of the auditory system [23]. This unit allows for a more accurate assessment of the actual nuisance experienced, as noise is now recognized as one of the most threatening environmental factors for urban health [24].

Noise disturbance generates irritability and anxiety. In children exposed in schools, it results in reading difficulties and a decline in academic performance. Noise thus degrades human capital, particularly in cities in developing countries [25] [26].

Sub-Saharan Africa is experiencing one of the strongest urbanization dynamics in the world. Studies in several cities (Lagos, Accra, Abidjan) reveal L_{Aeq} equivalent levels exceeding 80 to 90 dB(A) in some intersections, well above the WHO threshold of 70 dB(A) for commercial areas [27]-[29].

1.1.2. The Footprint of Noise Pollution in Ivory Coast

In Côte d'Ivoire, the impact of noise pollution has become a major environmental and public health concern. The in-depth study conducted on the Ivorian urban environment shows that the infrastructure deficit in the face of transport demand, coupled with an aging vehicle fleet estimated at over 800,000 vehicles in Abidjan, generates extreme levels of noise and pollution [30].

Endemic traffic congestion and driver behavior (excessive use of horns) exacerbate this nuisance. The disturbance is so significant that noise is one of the main sources of citizen complaints recorded by the Sanitation and Public Health Brigade (BAS). Official statistics reveal that purely residential neighborhoods are not spared: the Cocody district, for example, accounts for 41% of complaints in the economic capital, reflecting the conflicts of use created by the proliferation of informal eateries, bars, and places of worship within residential areas (BAS, 2022). This dynamic of urban noise dispersal observed in Abidjan [31] is now tending to be replicated with the same intensity in major cities in the interior of the country.

The Ivorian state has [32] setting strict thresholds according to the type of zone, reinforced by [33] the Hygiene Code. However, its application is hampered by the realities on the ground. In Man, "the city of 18 mountains," the basin-like topography promotes the reverberation of sound waves off the hills, amplifying the acoustic accumulation in congested intersections [34] [35].

The acoustic signal captured in urban environments is inherently random and non-stationary. To analyze it rigorously, a digital processing chain is necessary: digitization, filtering, spectral analysis, descriptor extraction, and statistical characterization.

The first step is to convert the analog pressure signal $p(t)$ into a digital signal $p[n]$. According to the Shannon-Nyquist theorem, the sampling frequency F_s must be at least twice the maximum frequency of the signal [36].

For urban acoustic signals, F_s = 44,100 Hz or 48,000 Hz is generally used, covering the entire audible spectrum. The digital signal is given by formula 2.

$$p[n] = p(n/F_s), n = 0,1,2,\cdots,N-1 \quad (2)$$

where N is the total number of samples. The recording time is $T = N/F_s$.

1.1.3. Sound Pressure Level and Energy Indicators

The instantaneous sound pressure level $L(t)$ expressed in decibels is given by formula 3.

$$L(t) = 10 \times \log_{10}\left(p^2(t)/p_0^2\right) \text{ with } p_0 = 20\,\mu\text{Pa} \quad (3)$$

The continuous equivalent level $L_{\text{Aeq},T}$, a key indicator for assessing discomfort over a period T, is defined by formula 4 [37] [38].

$$L_{\text{Aeq},T} = 10 \times \log_{10}\left(\frac{1}{T}\int_0^T p_A^2(t)/p_0^2\,\text{d}t\right)(\text{dB(A)}) \quad (4)$$

In practice, for N samples with weighting A, the relationship becomes (formula 5).

$$L_{\text{Aeq}} = 10 \times \log_{10}\left(\frac{1}{N}\sum_n p_A^2[n]/p_0^2\right)(\text{dB(A)}) \quad (5)$$

where $p_A[n]$ is the signal filtered by the A weighting. This indicator is the main parameter for comparison with WHO standards and Ivorian regulations.

In standard acoustics, analysis by octave or third-octave bands is recommended by standard [39]. For an octave band centered at f_c, the cutoff frequencies are:

$$f_{\text{inf}} = \frac{f_c}{\sqrt{2}} \text{ et } f_{\text{sup}} = f_c \times \sqrt{2} \text{ (octave band)}$$

$$f_{\text{inf}} = \frac{f_c}{2^{\frac{1}{6}}} \text{ et } f_{\text{sup}} = f_c \times 2^{\frac{1}{6}} \text{ (third oh an octave)}$$

The level per band is given by the following formula 6:

$$L_{\text{bande}} = 10 \times \log_{10}\left[\sum_{f_{\text{inf}}}^{f_{\text{sup}}} \frac{|P[k]|^2}{p_0^2}\right](\text{dB}) \quad (6)$$

The center frequencies normalized in third octaves cover from 20 Hz to 20 kHz, with 31 bands in total.

1.1.4. Statistical Indicators (Percentiles L_n)

The statistical distribution of sound levels allows us to characterize the temporal variability of the noise. The percentile L_n is the sound level exceeded n% of the measurement time, defined by formula 7 [40]:

$$P(L > L_n) = \frac{n}{100} \quad (7)$$

The practical indicators are:

- L_{10}: level exceeded 10% of the time indicates repeated peaks (vehicle traffic).
- L_{50}: median level represents the average perceived noise.
- L_{90}: residual background noise level in the absence of notable events.

- L_{99}: level exceeded 1% of the time represents extreme peaks.

The acoustic dynamics D of the site is defined by formula 8 as:

$$D = L_{10} - L_{90}\,(\mathrm{dB}) \tag{8}$$

1.2. Shape Descriptors: ZCR and Spectral Centroid

The Zero Crossing Rate (ZCR), defined by formula 9, measures the frequency at which the signal changes sign and provides information on the tone or noise of the signal.

$$\mathrm{ZCR} = \frac{1}{2N} \times \sum_n \left|\mathrm{sgn}\, p[n] - \mathrm{sgn}\, p[n-1]\right| \tag{9}$$

A high ZCR indicates a signal rich in high frequencies (broadband noise), while a low ZCR characterizes a tonal sound. The Spectral Centroid CS defined by formula 10 gives the frequency center of gravity of the signal [41]:

$$\mathrm{CS} = \frac{\sum_k k \times \left|P[k]\right|^2}{\sum_k \left|P[k]\right|^2}\,(\mathrm{Hz}) \tag{10}$$

These combined descriptors allow for the automatic classification of acoustic sources (road traffic, market, horn, amplified music) by machine learning.

Digital filtering is a key step in applying standardized A-weighting. The frequency response of the A-weighted filter is defined by formula 11 [42].

$$(f) = \frac{12194^2 \times f^4}{\left(f^2 + 20.6^2\right) \times \sqrt{f^2 + 107.7^2} \times \sqrt{f^2 + 737.9^2} \times \left(f^2 + 12194^2\right)} \tag{11}$$

The level in dB(A) is $A(f) = 20\log_{10}(RA(f)) + 2.00$. In the digital domain, this filter is implemented as a 4th-order IIR (Infinite Impulse Response) filter [43].

2. Materials and Methods

2.1. Equipment

In this study, the equipment used consists of three main elements: a smartphone serving as a sound capture device, MATLAB software for data processing, and a set of recording parameters defined beforehand to ensure the reproducibility of the measurements.

The acoustic recordings were made using a Samsung Galaxy A13 smartphone, shown in **Figure 3**. This choice was motivated by the device's availability, its portability in the field, and the sufficient quality of its integrated microphone to capture sound signals in the frequency ranges studied. The smartphone was running Android 14, and the recording application used was Voice Recorder version 21.4.51.51.

Although this type of device has limitations compared to dedicated professional equipment (such as certified sound level meters), it was deemed suitable for the exploratory context of this study.



Figure 3. Samsung Galaxy A13 smartphone used for acoustic recordings.

To ensure consistency between the different measurement sessions, fixed recording parameters were defined and systematically applied to all measurement points. These parameters are summarized in **Table 1**.

Table 1. Acoustic recording parameters used during field measurement campaigns.

Setting	Value retained
Sampling frequency	44,100 Hz
Audio format	M4A
Duration per recording	20 seconds
Microphone height	1.20 m from the ground
Profit management	Automatic (generated by the native Samsung application)
Measurement weather conditions	No rain, light wind, sunny

The sampling frequency of 44,100 Hz was chosen because it covers the entire human audible spectrum (20 Hz - 20 kHz).

2.2. Method

2.2.1. Study Area

The study area is the city of Man (**Figure 4**), capital of the Tonkpi region, located in western Ivory Coast.

This is a medium-sized urban city characterized by sustained economic and commercial activity, as well as relatively heavy road traffic along its main thoroughfares. Measurement points were selected primarily along the city's main roads, as, according to [44], road traffic is the primary source of noise in urban areas. Areas near high-traffic roads are indeed those where noise levels are highest and where the dis-

turbance is most acutely felt by local residents, with documented health effects such as high blood pressure, sleep disturbances, and irritability [45] [46]. Furthermore, in urban areas, road traffic is the main source of noise pollution [47], and noise levels measured near arterial roads regularly exceed recommended thresholds during peak hours, fully justifying the targeting of these areas in this study.

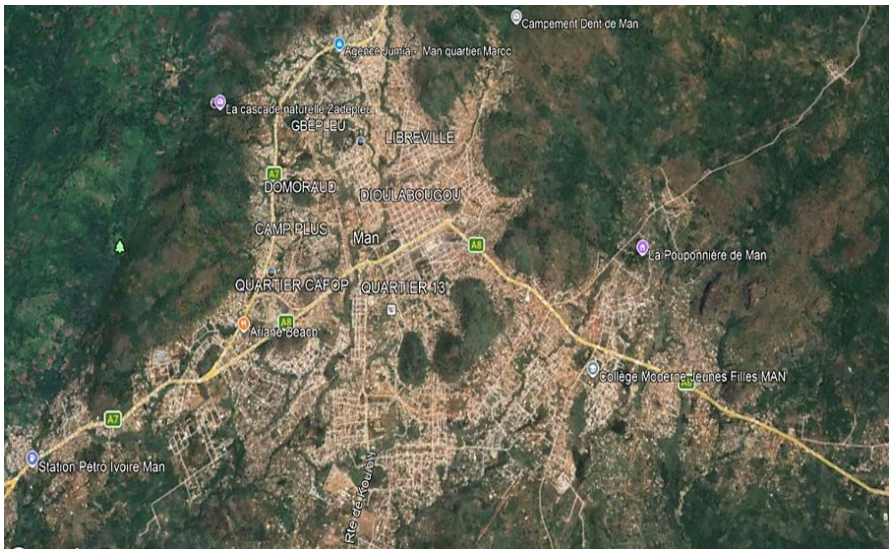


Figure 4. Satellite image of the city of Man.

Five neighborhoods representative of Man's urban diversity were selected: Sari (at a road intersection), Capen (industrial zone), Commerce, Dioulaboubou, and Domoraud (**Figure 5**). This selection allows for the coverage of different types of urban acoustic environments, ranging from high-traffic intersections and industrial zones to neighborhoods with a commercial and residential focus.



Figure 5. Satellite image and measurement point of the Domoraud district.

2.2.2. Measurement Protocol

The measurement campaign took place over several days, covering three types of

days: a weekday (Monday), a midweek day (Thursday), and a rest day (Sunday). This choice aims to capture the variability of road traffic according to the day of the week, as mobility patterns differ significantly between weekdays and Sundays. For each site, we chose three periods of the day that correspond to the times when there is the most activity in the city:

- 9 AM (morning period, corresponding to peak hours and the near opening of commercial activities);
- 12 PM (midday period, marked by heavy road and commercial activity);
- 5 PM (evening period).

The smartphone was held at a height of approximately 1.20 m above the ground, in accordance with practices adopted in similar studies [48] [49], away from obstacles that could disrupt sound propagation. Measurements were taken in calm weather, in the absence of strong winds or rain, to minimize meteorological interference with the captured signal (Table 2).

Table 2. Summary of the measurement protocol.

Settings	Values
City of study	Man, Tonkpi region, Ivory Coast
Neighborhoods studied	Sari, Capen, Commerce, Dioulaboubou, Domoraud
Zone type	Urban (main road axes)
Measurement days	Monday, Thursday and Sunday
Time slots	9 AM, 12 PM, 5 PM
Microphone height	1.20 m from the ground
Weather conditions	No rain, light wind, sunny

2.2.3. Sound Level Calculation and Calibration

The A-weighted instantaneous sound level, denoted $L_A(t)$, was calculated by applying a FAST time integration constant (125 ms), in accordance with the requirements of IEC 61672-1 for sound level meters. Since the raw data captured by the smartphone's microphone (Samsung Galaxy A13) is expressed in dBFS, a calibration step is required to estimate the actual sound pressure level in dB(A) SPL. The relationship between the digital level and the acoustic physical quantity is modeled by the linear transfer equation $L_{\text{Physics}} = L_{\text{digital}} + C$, validated by work on smartphone metrology [50], where L_{Physics} denotes the final sound pressure level in dB(A) SPL, L_{digital} the effective RMS level of the dBFS-weighted signal, and C the calibration constant specific to the device. In the absence of in situ calibration by pistonphone, this constant was empirically set at $C = 110$ dB, a value justified on the one hand by the nominal sensitivity of MEMS sensors which, generally exhibiting -26 dBFS for 1 Pascal either 94 dB SPL [51], place the theoretical saturation point around 120 dB SPL, and on the other hand by the need to compensate for the software pre-amplification gain of approximately +10 dB applied natively by

Android, whose NIOSH studies confirm that the empirical offset correction makes it possible to obtain a coherent sound pressure level representative of the sound environment studied [52].

Two additional nuisance indices were calculated from the basic indicators, in accordance with the formulas established in the literature [53]:

- The Noise Pollution Level (L_{NP}), which integrates both the average level and the fluctuation of the signal, is given by formula 12:

$$L_{NP} = L_{50} + \frac{\left(L_{10} - L_{90}\right)^2}{60} + \left(L_{10} - L_{90}\right) \tag{12}$$

- The Traffic Noise Index (TNI), which further weights signal fluctuation and constitutes an indicator of annoyance specifically related to road traffic, is given by formula 13.

$$\mathrm{TNI} = 4 \times \left(L_{10} - L_{90}\right) + L_{90} - 30 \tag{13}$$

These two indices are represented as grouped bar charts for each time period, allowing a direct comparison of noise levels between different times of day. A TNI above 74 dB(A) is considered the threshold for significant disturbance according to current standards [54].

3. Results and Discussion

3.1. Acoustic Results by Zone (Neighborhood)

This section presents all the acoustic descriptors calculated for each of the five studied neighborhoods, at the three selected time periods (9 a.m., 12 p.m., and 5 p.m.). For each site, a table groups all the acoustic, statistical, psychoacoustic indicators and signal descriptors. **Tables 3-5** present the indicators and descriptors. Signal obtained respectively for the Sari, Capen and Commerce districts.

Table 3. Indicators and descriptors signal obtained for the SARI district.

Indicators and Descriptors	Sari 9 AM	Sari 12 h	Sari 5 PM
Acoustic indicators			
L_{Aeq} (dB)	70.56	72.55	71.53
L_{Zeq} (dB)	83.27	84.94	84.62
L_{Ceq} (dB)	77.68	79.32	79
L_{Cpeak} (dB)	91.74	95.89	94.92
L_{AFmax} (dB)	75.36	84.16	78.96
Statistical indicators			
L_{10} (dB)	72.74	74.82	74.17
L_{50} (dB)	69.88	70.35	70.39
L_{90} (dB)	68.13	67.78	68.69

Continued

Psychoacoustic indicators			
Loudness (Sones)	28	29.06	29.71
Loudness Level (Phons)	88.08	88.61	88.93
Signal descriptors			
Dynamic range (dB)	4.6	7.03	5.48
Energy	103.3	165.2	130.63
RMS value	0.0107	0.0134	0.0119
ZCR	0.078	0.0758	0.084
Mean SC (Hz)	2377.8	2307.76	2439.64
Low/Total (%)	11.77	10.65	13.05
Mid/Total (%)	67.74	49.73	62.48

Table 4. Signal indicators and descriptors obtained for the Capen district.

Indicators and Descriptors	Capen 9 AM	Capen 12 PM	Capen 5 PM
Acoustic indicators			
L_{Aeq} (dB)	66.09	69.45	62.62
L_{Zeq} (dB)	81.04	81.54	77.98
L_{Ceq} (dB)	75.38	75.88	72.35
L_{Cpeak} (dB)	94.99	96.05	91.38
L_{AFmax} (dB)	72.67	72.88	68.6
L_{AFmin} (dB)	56.55	63.20	57.28
Statistical indicators			
L_{10} (dB)	68.7	70.84	64.78
L_{50} (dB)	65.78	69.39	61.85
L_{90} (dB)	59.63	67.48	60.2
Psychoacoustic indicators			
Loudness (Sones)	20.56	26.17	16.47
Loudness Level (Phons)	83.62	87.10	80.42
Signal descriptors			
Dynamic range (dB)	9.08	3.36	4.58
Energy	36.18	79.4	16.57
RMS value	0.0064	0.0094	0.0043

Continued

ZCR	0.1019	0.1045	0.0712
Mean SC (Hz)	2616.43	2609.37	2172.78
Low/Total (%)	21.98	9.58	25.68
Mid/Total (%)	43.88	43.73	60.64
High/Total (%)	34.14	46.69	13.68

Table 5. Signal indicators and descriptors obtained for the commerce district.

Indicators and Descriptors	Shops 9 AM	Trade 12 PM	Shops 5 PM
Acoustic indicators			
L_{Aeq} (dB)	69.59	69.12	72.69
L_{Zeq} (dB)	82.63	86.03	84.53
L_{Ceq} (dB)	77.01	80.28	78.94
L_{Cpeak} (dB)	93.72	92.44	94.3
L_{AFmax} (dB)	76.75	74.43	81.39
L_{AFmin} (dB)	64.64	65.79	65.44
Statistical indicators			
L_{10} (dB)	71.61	70.72	75.84
L_{50} (dB)	68.78	68.57	71.32
L_{90} (dB)	66.78	67.29	68.03
Psychoacoustic indicators			
Loudness (Sones)	25.22	25.58	29.45
Loudness Level (Phons)	86.56	86.77	88.8
Signal descriptors			
Dynamic range (dB)	4.83	3.43	7.82
Energy	81.08	73.53	168.55
RMS value	0.0095	0.009	0.0136
ZCR	0.0662	0.0614	0.0725
Mean SC (Hz)	2120.67	2041.46	2233.97
Low/Total (%)	10.86	28.86	7.8
Mid/Total (%)	73.48	59.79	73.71
High/Total (%)	15.66	11.35	18.49

3.2. Results of the Acoustic Modeling

We have deepened the acoustic analysis of the data through three complementary models aimed at characterizing the temporal dynamics, the level of nuisance and the spectral signature.

The modeling of the temporal evolution (Figure 6) highlights a near-permanent acoustic saturation at the Sari crossroads.

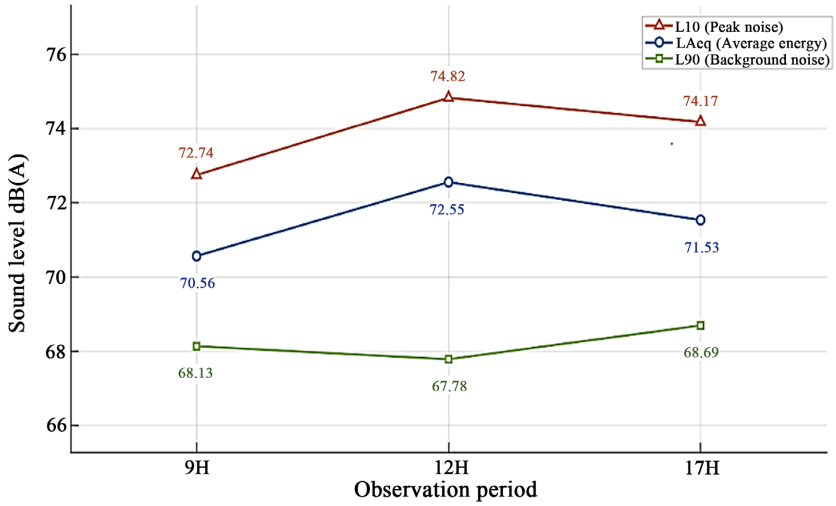


Figure 6. Temporal profile of the acoustic environment (Sari).

The L_{Aeq} at 9 a.m. is 70.56 dB(A), the L_{10} reaches 72.74 dB(A), and the L_{90} is at 68.13 dB(A), resulting in a dynamic range of 4.60 dB. At 12 p.m., this increases to 72.55 dB(A), the L_{10} to 74.82 dB(A), and the L_{90} drops slightly to 67.78 dB(A), for a dynamic range of 7.03 dB. At 5 p.m., the L_{Aeq} drops again to 71.53 dB(A), the L_{10} to 74.17 dB(A), and the L_{90} rises to 68.69 dB(A), with a dynamic range of 5.48 dB.

Figure 7 shows the intra-measurement evolution of the $L_A(t)$ signal at 12 h, the time range corresponding to the daily peak of L_{Aeq}.

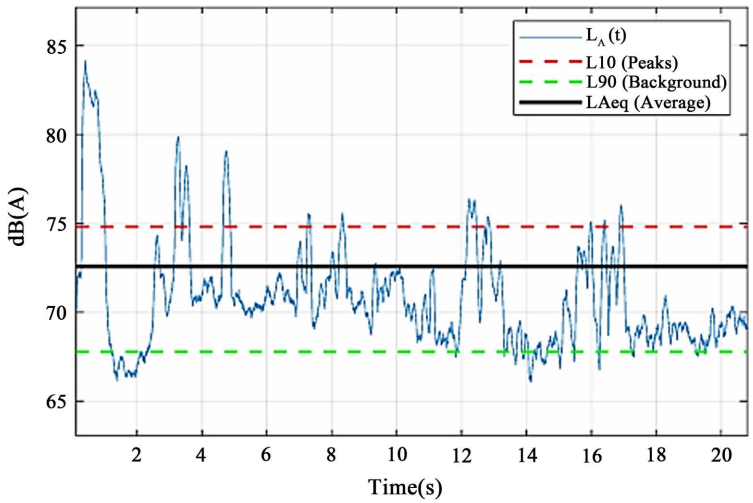


Figure 7. Time evolution of sound level $L_A(t)$ at 12 h.

The calculation of derived indices made it possible to assess the disruption caused by road traffic in the Sari district (Figure 8).

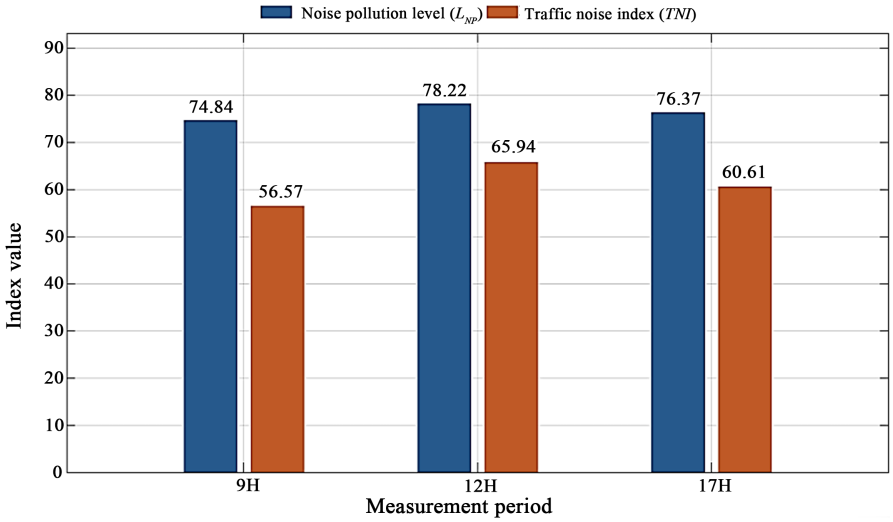


Figure 8. Comparison of noise nuisance indices in the sari district.

The L_{NP} recorded the following values in Sari: 74.84 at 9 AM, 78.22 at 12 PM, and 76.37 at 5 PM, while the TNI displayed 56.57 at 9 AM, 65.94 at 12 PM, and 60.61 at 5 PM. In both cases, 12 PM recorded the highest values, while 9 AM showed the lowest.

Figure 9 shows the energy distribution over the three frequency bands and the evolution of the spectral centroid at the three time slots.

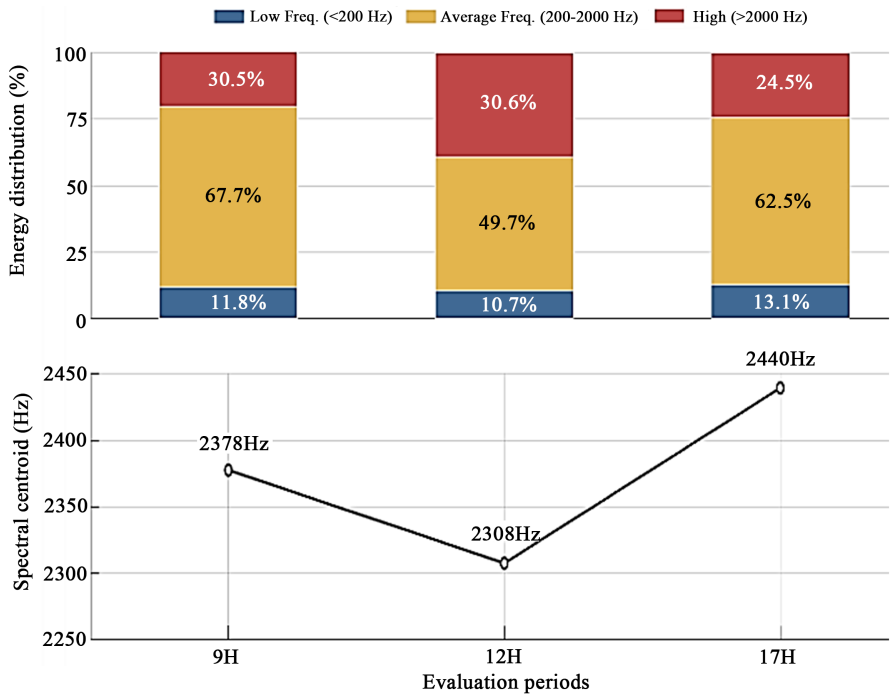


Figure 9. Acoustic and spectral signature of the sari crossroads.

At 9 a.m., mid-range frequencies dominated the spectrum (67.7%), while high (20.5%) and low (11.8%) frequencies shared the remainder asymmetrically. At noon, the balance shifted significantly: high frequencies increased sharply to 39.6%, at the expense of mid-range frequencies, which fell to 49.7%, while low frequencies remained almost stable at 10.7%. In the late afternoon, the morning pattern partially returned, with mid-range frequencies rising to 62.5% and high frequencies dropping to 24.5%, while low frequencies reached their highest level of the day (13.1%).

The spectral centroid follows a trough trajectory: from 2378 Hz at 9 a.m., it drops to 2308 Hz at noon, then rises to its highest level at 5 p.m., reaching 2440 Hz (Figure 10).

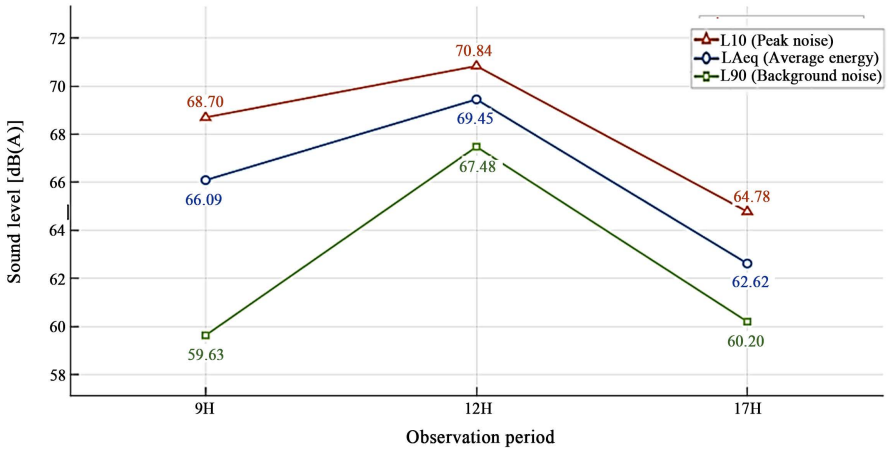


Figure 10. Temporal profile of the acoustic environment (Capen).

The L_{Aeq} levels at 9:00 (66.09 dB(A)), L_{10} (68.70 dB(A)), and L_{90} (59.63 dB(A)) exhibit a dynamic range of 9.08 dB. At 12:00, the three indicators converge (L_{Aeq} = 69.45 dB(A); L_{10} = 70.84 dB(A); L_{90} = 67.48 dB(A)), with a reduced dynamic range of 3.36 dB. At 17:00, all indicators decrease (L_{Aeq} = 62.62 dB(A); L_{10} = 64.78 dB(A); L_{90} = 60.20 dB(A)). Figure 11 shows the intra-measurement evolution of the $L_A(t)$ signal at 12:00, the time period corresponding to the daily peak of L_{Aeq}.

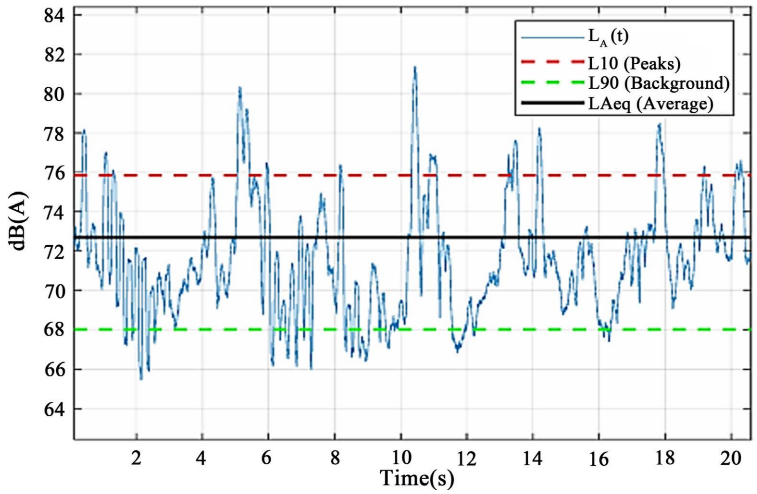


Figure 11. Temporal evolution of the sound level $L_A(t)$ at 12 PM.

The L_{NP} index recorded in Capen (Figure 12) was 76.22 at 9:00 AM, 72.94 at 12:00 PM, and 66.78 at 5:00 PM, indicating a downward trend throughout the day. The TNI index followed the same trend, with 65.91 at 9:00 AM, 50.92 at 12:00 PM, and 48.52 at 5:00 PM. The highest values for both indices were recorded at 9:00 AM, while the lowest values were recorded at 5:00 PM.

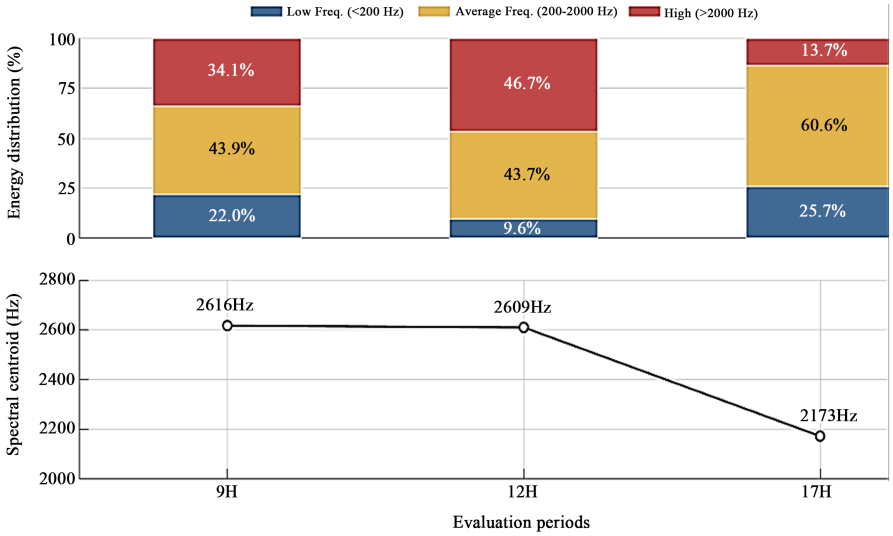


Figure 12. The acoustic and spectral signature of the Capen district.

The spectrum is immediately distinguished by a marked presence of high frequencies, which occupy 34.1% by 9 a.m., an unusually high level alongside mid-range frequencies (43.9%) and low frequencies (22.0%). At noon, high frequencies become even more prominent, peaking at 46.7%, while mid-range frequencies remain at 43.7% and low frequencies decline to 9.6%. By late afternoon, the trend reverses sharply: mid-range frequencies take over (60.6%), high frequencies fall to 13.7%, and low frequencies rise again to 25.7%.

The spectral centroid, stable between 9 AM and 12 PM (2616 Hz then 2609 Hz), shows a pronounced drop at the end of the day, falling to 2173 Hz at 5 PM.

At 9 a.m., the L_{Aeq} was 69.60 dB(A), the L_{10} reached 71.61 dB(A), and the L_{90} was 66.78 dB(A), resulting in a dynamic range of 4.83 dB ($L_{10} - L_{90}$). At 12 p.m., the L_{Aeq} decreased slightly to 69.10 dB(A), the L_{10} to 70.72 dB(A), and the L_{90} to 67.29 dB(A), with a reduced dynamic range of 3.43 dB. At 5 p.m., the L_{Aeq} reached its maximum value (72.70 dB(A)), accompanied by an L_{10} of 75.84 dB(A) and an L_{90} of 68.03 dB(A), with a dynamic range of 7.82 dB.

Figure 13 and Figure 14 show the intra-measurement evolution of the $L_A(t)$ signal at 5 PM, the time range corresponding to the daily peak of L_{Aeq} in the Commerce district.

In the trade sector, we observe the following readings: 74.00 at 9:00 AM, 72.20 at 12:00 PM, and 80.15 at 5:00 PM, with a dip at 12:00 PM before reaching its peak at 5:00 PM. The TNI follows a similar trend, with 56.10 at 9:00 AM, 51.01 at 12:00 PM, and 69.27 at 5:00 PM. 5:00 PM records the highest values for both indices, while 12:00 PM shows the lowest.

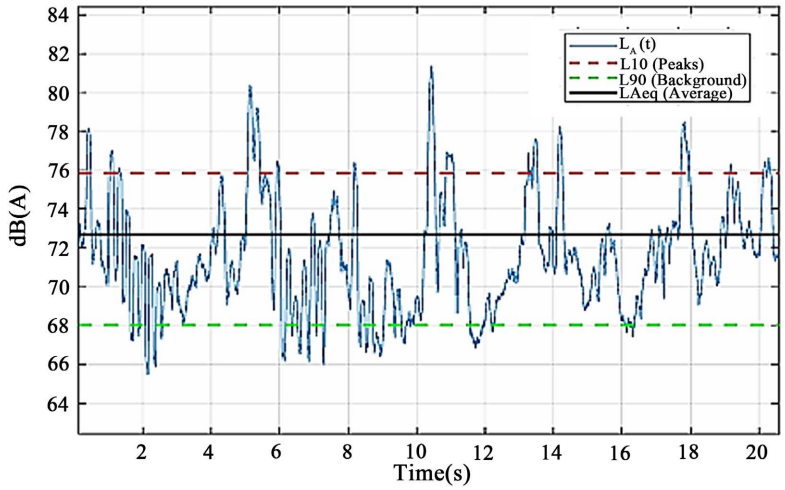


Figure 13. Temporal evolution of the $L_A(t)$ sound level at commerce (5 PM).

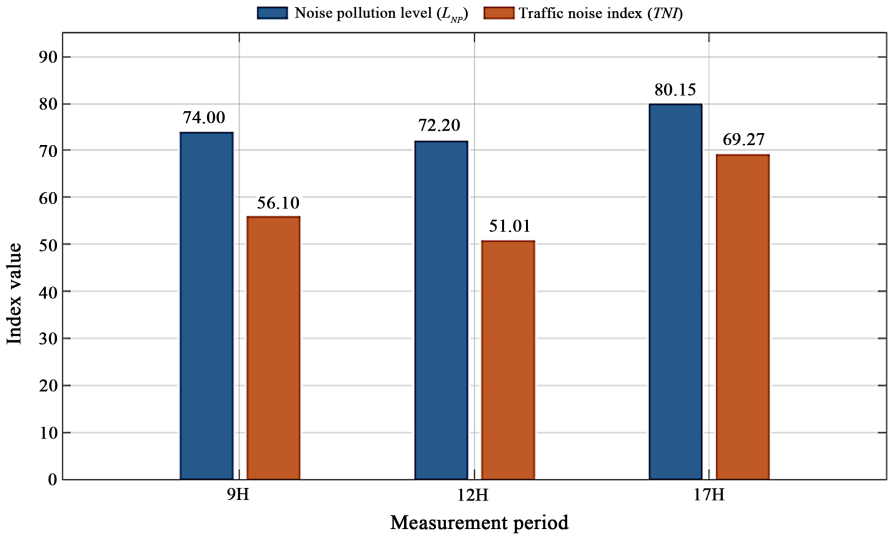


Figure 14. Comparison of noise nuisance indices in the commerce district.

Mid-range frequencies structure the spectrum throughout the day, clearly dominating at 9 a.m. (73.48%) and returning to a nearly identical level at 5 p.m. (73.71%), after a dip at noon (59.79%). It is precisely at this intermediate time that low frequencies momentarily take over, jumping to 28.86% compared to 10.86% in the morning, before falling back to 7.80% in the late afternoon. High frequencies, for their part, fluctuate within a more modest range, between 11.35% at noon and 18.49% at 5 p.m.

The spectral centroid follows a slightly valley trajectory: 2120.67 Hz at 9 a.m., 2041.46 Hz at noon, then 2233.97 Hz at 5 p.m., thus reaching its highest level at the end of the day.

The L_{Aeq} at 9:00 AM was 71.29 dB(A), the L_{10} reached 73.27 dB(A), and the L_{90} was 68.60 dB(A), resulting in a dynamic range of 4.67 dB ($L_{10} - L_{90}$). At 12:00 PM, it dropped slightly to 71.01 dB(A), the L_{10} rose to 73.70 dB(A), and the L_{90} fell to 67.20 dB(A), for a dynamic range of 6.50 dB. At 5:00 PM, it reached its daily max-

imum (72.41 dB(A)), accompanied by an L_{10} of 74.55 dB(A) and an L_{90} of 68.91 dB(A), with a dynamic range of 5.64 dB.

Figure 15 shows the intra-measurement evolution of the $L_A(t)$ signal at 17 h, the time range corresponding to the daily peak of L_{Aeq}.

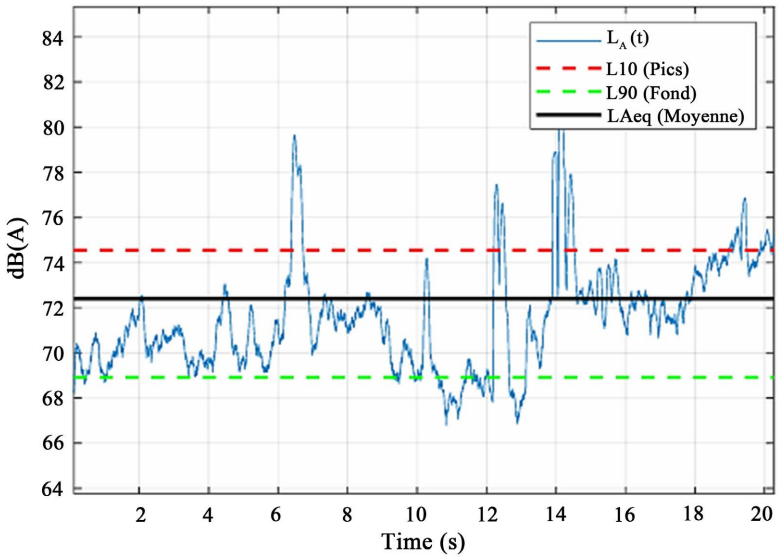


Figure 15. Temporal evolution of the $L_A(t)$ sound level at Dioulaboubou (5 PM).

Over this 20-second period (Figure 16), the $L_A(t)$ curve oscillates primarily between 66 and 80 dB(A). Two impulsive peaks clearly exceed L_{10} (74.55 dB(A)): a first peak around 6.5 s reaching approximately 79.5 dB(A), and a second around 14 s reaching approximately 80 dB(A). The signal briefly drops below the L_{90} threshold (68.91 dB(A)) between 10 and 12.5 s, reaching a minimum of approximately 66.5 dB(A). Outside this window, the curve remains mostly above L_{90}. The final phase (15 - 20 s) exhibits a higher average level than the initial phase (0 - 5 s), with several crossings of L_{10}.

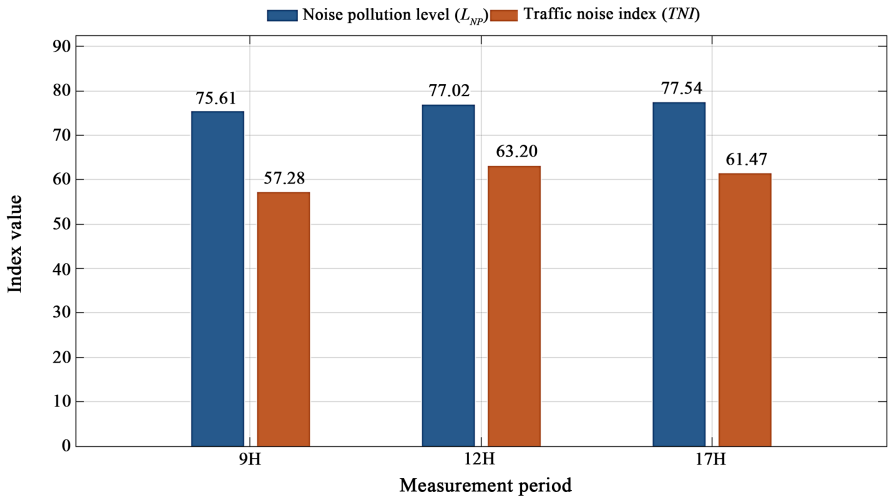


Figure 16. Comparison of noise nuisance indices in the Dioulabougou district.

For the Dioulaboubou district, the L_{NP} index recorded values of 75.61 at 9:00 AM, 77.02 at 12:00 PM, and 77.54 at 5:00 PM, showing a slight upward trend throughout the day. The TNI index followed the same trend, with values of 57.28 at 9:00 AM, 63.20 at 12:00 PM, and 61.47 at 5:00 PM, with a slight decrease between 12:00 PM and 5:00 PM. Both the L_{NP} and the TNI indexes recorded their highest values at 5:00 PM and 12:00 PM, while 9:00 AM showed their lowest values.

From 9 a.m. onwards, mid-range frequencies clearly dominate (63.33%), in a spectrum that is otherwise fairly balanced between low (17.52%) and high (19.15%) frequencies (Figure 17).

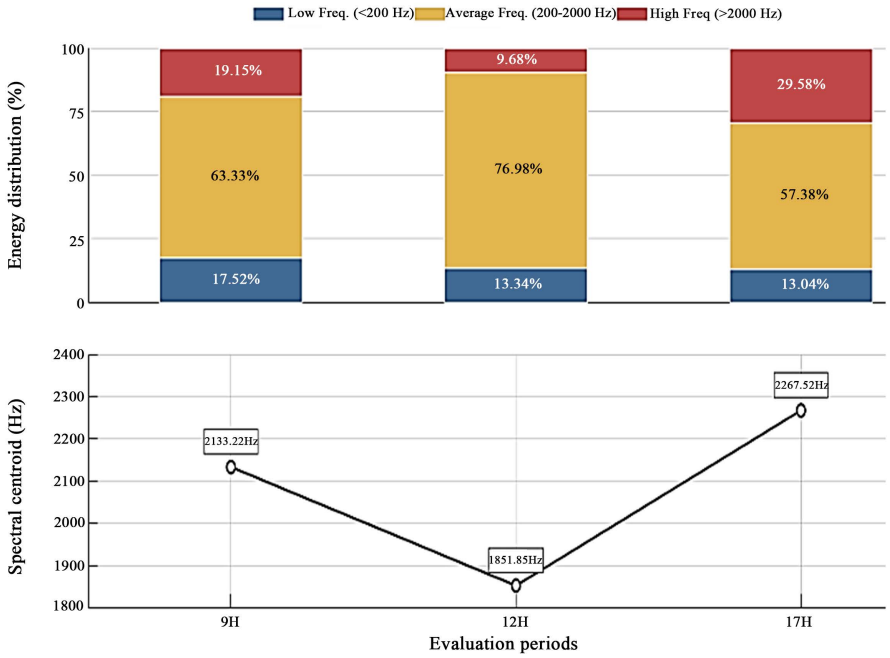


Figure 17. Acoustic and spectral signature of the Dioulaboubou district.

This polarization intensifies at midday, when mid-range frequencies reach their peak at 76.98%, while low frequencies drop to 13.34% and high frequencies to 9.68%. The trend then reverses: in the late afternoon, high frequencies experience a marked resurgence, jumping to 29.58%, at the expense of mid-range frequencies, which fall back to 57.38%, while low frequencies remain stable at 13.04%.

The spectral centroid, meanwhile, follows a contrasting trajectory. From 2133.22 Hz at 9 a.m., it drops to 1851.85 Hz at noon, before rising vigorously to 2267.52 Hz at the end of the day.

At 9 a.m., the L_{Aeq} is 66.95 dB(A), the L_{10} reaches 68.68 dB(A), and the L_{90} is at 62.47 dB(A), for a dynamic range $L_{10} - L_{90}$ of 6.21 dB. At 12 p.m., the L_{Aeq} rises to 67.87 dB(A), and the L_{10} to 69.87 dB(A).

dB(A) and L90 at 65.40 dB(A), for a reduced dynamic range of 4.47 dB. At 5 p.m., L_{Aeq} reached its daily maximum (69.29 dB(A)), accompanied by an L_{10} of 71.83 dB(A) and an L_{90} of 65.77 dB(A), with a dynamic range of 6.06 dB.

Figure 18 shows the intra-measurement evolution of the $L_A(t)$ signal at 17 h, the time range corresponding to the daily peak of L_{Aeq}.

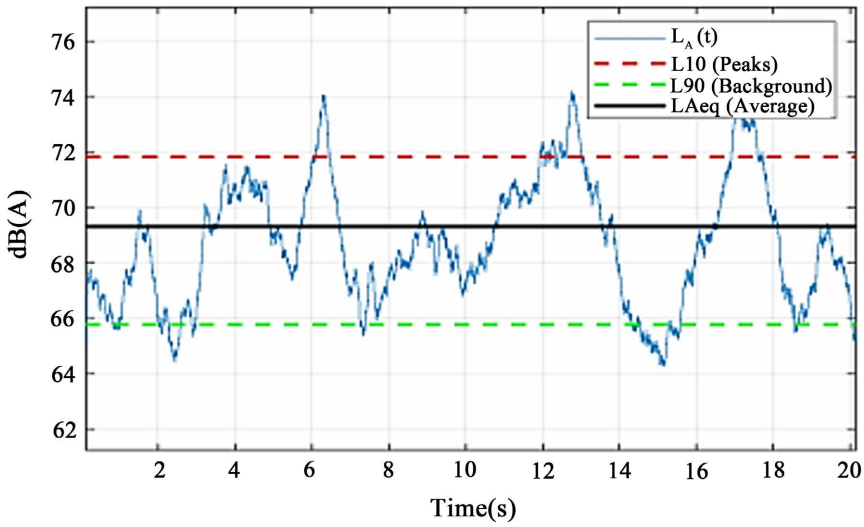


Figure 18. Temporal evolution of the $LA(t)$ sound level at Domoraud (5 PM).

At Domoraud, shown in Figure 19, the values recorded were 73.09 at 9 AM, 72.48 at 12 PM and 75.25 at 5 PM, with a slight decrease at 12 PM before reaching its maximum at 5 PM.

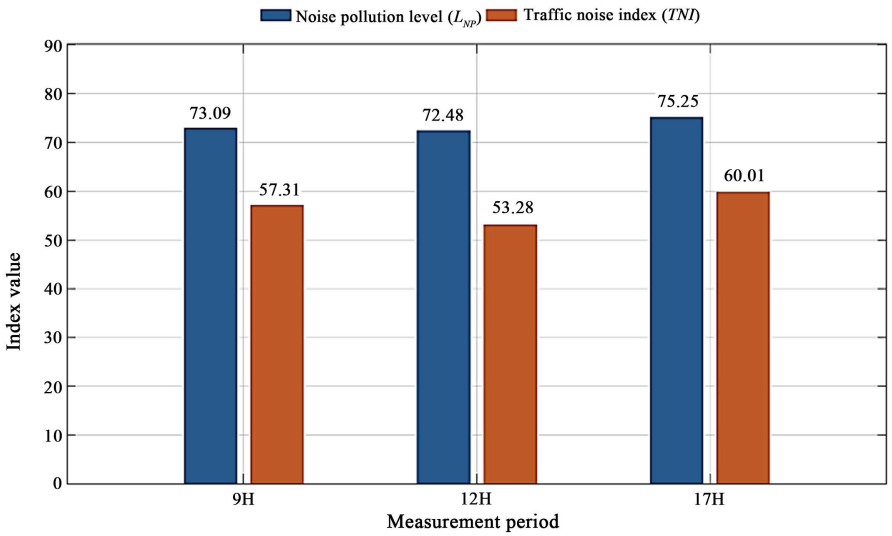


Figure 19. Comparison of noise nuisance indices in the Domoraud district.

The TNI follows the same trend with 57.31 at 9 AM, 53.28 at 12 PM and 60.01 at 5 PM. The 5 PM period records the highest values for both indices, while 12 PM shows the lowest values.

The day reveals a progressive concentration of energy towards mid-range frequencies. By 9 a.m., these already dominate the spectrum (56.70%), flanked in a relatively balanced way by low (24.25%) and high (19.05%) frequencies. This trend

intensifies at noon, with mid-range frequencies absorbing nearly three-quarters of the total energy (70.96%), while the two extremes diminish symmetrically. By late afternoon, the shift reaches its peak: mid-range frequencies reach 79.19%, relegating low frequencies to 12.99% and high frequencies to 7.82%.

The spectral centroid, meanwhile, remains remarkably stable throughout the day, staying between 1972 Hz at 12 PM and 1992 Hz at 9 AM, before stabilizing at 1983 Hz at 5 PM.

3.3. Discussion

3.3.1. Acoustic Exposure Levels and Compliance with Normative Standards

The first observation that stands out upon reading the results is the widespread and persistent transgression of normative thresholds across all the sites studied. The measured A-weighted continuous equivalent (L_{Aeq}) levels range from 66.95 dB(A) (Domoraud, 9 AM) to 72.70 dB(A) (Commerce, 5 PM), values that are systematically 12 to 18 decibels higher than the recommendations of the World Health Organization (WHO) and Ivorian regulations, which set the daytime threshold at 55 dB(A) in outdoor environments to protect public health [55]. This finding is all the more significant as it uniformly affects areas of different types: road intersection, industrial zone, dense commercial zone, residential zone, suggesting a pervasive acoustic saturation across the entire urban fabric of Man.

This result is consistent with the work of [56], who conducted a comparative study of noise levels in the cities of Ibadan and Ile-Ife, Nigeria. These authors report average noise levels ranging from 53 to 89 dB(A) depending on the type of land use zone, all categories combined, well above the limits authorized by the WHO, with the highest values recorded in commercial and transport areas. Similarly, [57], in a recent study of five sub-metropolises in Kumasi, Ghana, document noise levels ranging from 51.86 to 82.87 dB(A), with commercial areas recording the highest values, and find that all sites exceed the 2018 WHO guidelines on environmental noise. Both studies confirm that the widespread exceeding of normative thresholds in medium-sized African cities is a structural reality, and that accelerated urbanization and the growth of the vehicle fleet are the main explanatory factors.

From a health perspective, such levels of chronic exposure are associated, in the epidemiological literature, with documented health effects: high blood pressure, sleep disturbances, irritability, and decreased cognitive performance [58] [59]. The city of Man, whose basin-like topography promotes reverberation and the accumulation of sound waves on the surrounding hills, is in a position of structural acoustic vulnerability that further exacerbates the actual exposure of its inhabitants.

3.3.2. Temporal Variability of Acoustic Indicators as a Function of Land Use

Beyond absolute levels, temporal analysis of acoustic indicators reveals contrasting daily patterns, reflecting the functional nature of each neighborhood and the struc-

ture of human activities taking place there. The Sari neighborhood, a busy road intersection, exhibits a peak in L_{Aeq} at noon (72.55 dB(A)), a period corresponding to the maximum intensity of transit traffic. Commercial neighborhoods such as Commerce and Dioulaboubou record their highest levels in the late afternoon (5 PM), with L_{Aeq} reaching 72.70 and 72.41 dB(A) respectively, reflecting the resurgence of commercial activity and return traffic at the end of the day. The Capen industrial zone shows a peak at noon followed by a significant decrease at 5 PM (L_{Aeq} = 62.62 dB(A)), consistent with the rhythm of daytime activities. Finally, the residential area of Domoraud shows an increasing trend throughout the day, with a maximum at 5 PM (69.29 dB(A)), resulting from a progressive accumulation of traffic.

These observations are directly corroborated by the results of [60], who studied the diurnal variation of road traffic noise at five sites in the city of Makurdi, Nigeria. These authors report L_{Aeq} values of 68.65 to 70.46 dB(A) during the dry season, with distinct temporal modulation according to traffic pattern and land cover type. The convergence between the temporal profiles of Makurdi and those of Man, two medium-sized African cities with mixed economies, reinforces the idea that the daily dynamics of urban noise are largely determined by local socio-economic rhythms rather than purely physical site characteristics. [61] show that road traffic noise levels in Kahramanmaraş, Türkiye, vary according to land use type and time of day, with residential and mixed commercial areas recording the highest levels, while the minimum and maximum values are observed at midday and in the evening, respectively.

3.3.3. Assessment of Noise Pollution Using the L_{NP} and TNI Indices

Examining the derived noise pollution level (L_{NP}) and traffic noise index (TNI) provides a complementary and more nuanced understanding of the noise nuisance perceived by residents. The L_{NP} index exceeds 70 dB(A) in all neighborhoods and at all time periods. Even more significantly, the TNI reaches high values at the Sari intersection, in the Commerce district, and in the Dioulaboubou district, reflecting a nuisance linked to repeated fluctuations in the acoustic signal. The dynamic range $D = L_{10} - L_{90}$, between 3.36 dB (Capen, 12:00) and 9.08 dB (Capen, 9:00), confirms that certain sites experience marked acoustic variability, indicative of repeated impulsive sound events characteristic of heavy traffic.

The comparison with the data from [62] is particularly instructive: these authors report L_{NP} values for Makurdi ranging from 62.90 to 67.64 dB(A) during the dry season, levels significantly lower than the L_{NP} measured in Man, which exceeds 73 dB(A) in all neighborhoods. This difference reveals that noise pollution in Man is significantly higher than in a comparable Nigerian city in terms of size and activity, reinforcing the need for targeted regulatory intervention. In a different context, focusing on major road intersections in the city of Cox's Bazar in Bangladesh, [63] show that TNI values frequently exceed tolerable dissatisfaction thresholds, with 19 out of 105 time slots exhibiting extreme levels of dissatisfaction, and that

residents associate this exposure with health effects such as irritation (84.44%), headaches (62.37%), and cognitive impairment (44.44%).

3.3.4. Spectral Characterization of the Urban Sound Environment

Analysis of the energy distribution of the acoustic signal between low, mid, and high frequencies reveals a consistent dominance of mid-frequencies (200-2000 Hz) across all five neighborhoods and during all time periods studied. This spectral range encompasses the contributions of engine noise, rolling noise, and aerodynamic interactions, which constitute the characteristic spectral components of motorized road traffic. The spectral centroid, located between 1851 Hz (Dioulaboubou, 12 AM) and 2616 Hz (Capen, 9 AM), is consistently situated within the mid-to-high frequency range, corroborating the identification of traffic as the primary source.

This spectral configuration is consistent with the reference data of [64], according to which urban road noise in developing countries produces equivalent levels of 75 to 80 dB(A) over 24 hours along high-traffic roads, with energy mainly concentrated in the mid-frequency bands. This finding is also consistent with the results of [65], which attribute most of the noise pollution observed in Nigerian cities to vehicle traffic on roads and commercial routes. The temporal modulation of the spectral centroid, for example, the drop from 2616 Hz at 9:00 AM to 2173 Hz at 5:00 PM in Capen, or the rise observed in Dioulaboubou at the end of the day, indicates variations in the composition of noise sources throughout the day, which may reflect changes in the type of vehicles (heavy goods vehicles in the morning, two-wheelers in the afternoon) or in the commercial activities along the roads.

4. Conclusions and Outlook

The aim of this study was to analyze and model urban noise in five representative districts of the city of Man (Sari, Capen, Commerce, Dioulaboubou and Domoraud) by digital processing of the acoustic signal, in order to objectively assess the levels of noise exposure of the populations and to formulate concrete recommendations for the local authorities.

The sound recordings were made using a Samsung Galaxy A13 smartphone at three time slots (9 AM, 12 PM and 5 PM) on three types of days (weekday, midweek and rest), then processed under MATLAB through a digital chain reproducing the functions of a Class 2 sound level meter. This chain made it possible to calculate a complete set of acoustic indicators (L_{Aeq}, L_{10}, L_{50}, L_{90}, L_{Cpeak}, L_{NP}, TNI, loudness in Sones and Phons) and spectral descriptors (spectral centoid, energy distribution by frequency bands), organized around three complementary models: temporal description, nuisance index and spectral.

The results reveal widespread noise saturation throughout the urban fabric of Man. L_{Aeq} levels range from 66.95 dB(A) in Domoraud to 72.70 dB(A) in the Commerce district, exceeding the daytime threshold of 55 dB(A) recommended by the WHO and Ivorian decree no. 2016-791 by 12 to 18 dB(A), without exception for

any particular site or time period. Spectral analysis confirms the predominance of motorized traffic as the main noise source, with mid-range frequencies (200 - 2000 Hz) representing between 43.9% and 79.2% of the total acoustic energy. Each district also exhibits a distinct temporal profile consistent with its functional purpose: a peak at noon at the Sari intersection, a peak at 5 p.m. in the Commerce and Dioulaboubou commercial areas, a decrease in the evening in Capen, and a continuous increase in Domoraud. All of these observations fully confirm the four research hypotheses formulated in the introduction.

Faced with this worrying situation, several recommendations are essential for decision-makers: strict regulation of the use of horns, establishment of low-traffic zones, stricter technical inspections of aging vehicles, and integration of acoustic requirements into urban planning documents. Further studies, including nighttime measurements, calculation of the Lden index, and a residents' perception survey, would allow for a more in-depth analysis of these findings and refine urban noise management policies.

Author Contributions

All authors contributed to the conduct of this study and the preparation of the manuscript. All have approved the final version of the article.

Conflicts of Interest

The authors declare no conflicts of interest regarding the publication of this paper.

References

[1] WHO (2018) Environmental Noise Guidelines for the European Region. World Health Organization Regional Office for Europe, 180 p.

[2] Van Kempen, E., Casas, M., Pershagen, G. and Foraster, M. (2018) WHO Environmental Noise Guidelines for the European Region: A Systematic Review on Environmental Noise and Cardiovascular and Metabolic Effects: A Summary. *International Journal of Environmental Research and Public Health*, **15**, Article 379. https://doi.org/10.3390/ijerph15020379

[3] Clark, C. and Paunovic, K. (2018) WHO Environmental Noise Guidelines for the European Region: A Systematic Review on Environmental Noise and Quality of Life, Wellbeing and Mental Health. *International Journal of Environmental Research and Public Health*, **15**, Article 2400. https://doi.org/10.3390/ijerph15112400

[4] Smith, B.J., Peters, R.J. and Hollins, M. (2011) Acoustics and Noise Control. 3rd Edition, Routledge, 312 p.

[5] Laurore (2022) Sanitation and Hygiene—3018 Noise Nuisances Recorded by the Sanitation and Hygiene Brigade in Abidjan. https://www.laurore.net/assainissement-et-salubrite-3018-nuisances-sonores-recensees-par-la-brigade-de-lassainissement-et-de-la-salubrite-a-abidjan/

[6] Sylla, G. (2024) Pollutions atmosphérique et sonore en milieu urbain: le cas d'Abidjan (Côte d'Ivoire). Thèse de doctorat en études urbaines, Université du Québec, Institut national de la recherche scientifique (INRS), Centre Urbanisation Culture Société, 206 p. https://espace.inrs.ca/id/eprint/15582/

[7] Kang J. (2006) Urban Sound Environment. CRC Press, 304 p.

[8] Erfanian, M., Mitchell, A.J., Kang, J. and Aletta, F. (2019) The Psychophysiological Implications of Soundscape: A Systematic Review of Empirical Literature and a Research Agenda. *International Journal of Environmental Research and Public Health*, **16**, 3533. https://doi.org/10.3390/ijerph16193533

[9] Ziani, A. (2022) Cours d'acoustique architecturale (Course in Architectural Acoustics). Polycopié pédagogique destiné aux étudiants de Master 1 en architecture, Faculté de Technologie, Département d'architecture, Université Tahri Mohamed de Béchar, Algérie, année universitaire 2021-2022.

[10] Jedidi, M. and Soussi, C. (2013) Building Acoustics: Course and Solved Exercises. Édilivre, 148 p.

[11] Bouzir Tallal, A.K. (2018) Urban Morphology and Noise Pollution: A Cause-and-Effect Study. The Case of the City of Biskra. Ph.D. Thesis, Mohamed Khider University—Biskra, 215 p.

[12] Salomons, E.M. and Berghauser Pont, M. (2012) Urban Traffic Noise and the Relation to Urban Density, Form, and Traffic Elasticity. *Landscape and Urban Planning*, **108**, 2-16. https://doi.org/10.1016/j.landurbplan.2012.06.017

[13] Hagopian, E.J. and Machi, J. (2014) Abdominal Ultrasound for Surgeons. Springer, 187 p.

[14] Munot, P. and Nève, F.X. (2002) An Introduction to Phonetics: A Manual for Linguists, Speech Therapists and Speech-Language Pathologists. CEFAL Editions, 164 p.

[15] Shipman, J., Wilson, J.D. and Higgins, C.A. (2012) An Introduction to Physical Science. 13th Edition, Cengage Learning, 840 p.

[16] Halliday, D., Resnick, R. and Walker, J. (2018) Fundamentals of Physics. 11th Edition, Wiley.

[17] Giancoli, D.C. (1993) General Physics: Volume 3, Waves, Optics and Modern Physics. De Boeck-Wesmael, 488 p.

[18] Val, M. (2008) Lexicon of Acoustics: Architecture, Environment, Music. Le Harmattan, 126 p.

[19] Brau, A. (2013) Introduction to Acoustics and Its Applications: Course and Corrected Exercises. De Boeck Supérieur, 224 p.

[20] Hamayon, L. (2013) Achieving the Acoustics of a Building: Architectural Design, Sound Insulation and Acoustic Correction. Le Moniteur.

[21] Clark, C. and Paunovic, K. (2018) WHO Environmental Noise Guidelines for the European Region: A Systematic Review on Environmental Noise and Cognition. *International Journal of Environmental Research and Public Health*, **15**, 285. https://doi.org/10.3390/ijerph15020285

[22] Berglund, B., Lindvall, T. and Schwela, D. H. (Eds.) (1999) Guidelines for Community Noise. World Health Organization (WHO), 141 p. https://www.who.int/publications/i/item/a68672

[23] Amous, E. (2008) Sound and Noise. Master's Thesis, École Nationale Supérieure de Création Industrielle (ENSCI), 65 p.

[24] Jarosińska, D., Héroux, M., Wilkhu, P., Creswick, J., Verbeek, J., Wothge, J., *et al.* (2018) Development of the WHO Environmental Noise Guidelines for the European Region: An Introduction. *International Journal of Environmental Research and Public Health*, **15**, Article 813. https://doi.org/10.3390/ijerph15040813

[25] Zannin, P.H.T., Diniz, F.B. and Barbosa, W.A. (2002) Environmental Noise Pollution

in the City of Curitiba, Brazil. *Applied Acoustics*, **63**, 351-358. https://doi.org/10.1016/s0003-682x(01)00052-4

[26] UN-Habitat (2022) World Cities Report 2022: Envisaging the Future of Cities. United Nations Human Settlements Programme (UN-Habitat), 412 p. https://unhabitat.org/sites/default/files/2022/06/wcr_2022.pdf

[27] Sylla, G., Apparicio, P., Gelb, J. and Robin, O. (2025) Mapping Road Traffic Noise Descriptors in a Sub-Saharan City: An Extensivae Mobile Data Collection in Abidjan (ivory Coast). *African Transport Studies*, **3**, 100067. https://doi.org/10.1016/j.aftran.2025.100067

[28] Gnamien, S., *et al*. (2023) Chemical Characterization of Urban Aerosols in Abidjan and Korhogo.

[29] World Health Organization Regional Office for Europe (2009) Night Noise Guidelines for Europe. WHO Regional Office for Europe.

[30] Kouamé, P.K., Galli, A., Peter, M., Loss, G., Wassa, D., Bonfoh, B., *et al*. (2021) Access to Water and Sanitation Infrastructures for Primary Schoolchildren in the South-Central Part of Côte d'Ivoire. *International Journal of Environmental Research and Public Health*, **18**, Article 8863. https://doi.org/10.3390/ijerph18168863

[31] N'Guessan, B.V.H., *et al*. (2021) Estimation and Mapping of Air Pollutants in the City of Abidjan.

[32] Pellerin, G. (2006) Course in Architectural Acoustics. National Conservatory of Arts and Crafts (CNAM).

[33] Proakis, J.G. and Manolakis, D.K. (1996) Digital Signal Processing: Principles, Algorithms and Applications. 3rd Edition, Prentice-Hall International, 1000 p.

[34] ISO 1996-1 (2016) Acoustics—Description, Measurement and Assessment of Environmental Noise—Part 1: Basic Quantities and Assessment Procedures. International Organization for Standardization (ISO).

[35] IEC 61260-1 (2014) Electroacoustics—Octave-Band and Fractional-Octave-Band Filters—Part 1: Specifications. International Electrotechnical Commission (IEC).

[36] ISO 1996-2 (2017) Acoustics—Description, Measurement and Assessment of Environmental Noise—Part 2: Determination of Sound Pressure Levels. International Organization for Standardization (ISO).

[37] Peeters G. (2004) A Large Set of Audio Features for Sound Description (Similarity and Classification) in the CUIDADO Project. IRCAM Technical Report, Version 1.0, 25 p.

[38] IEC 61672-1 (2013) Electroacoustic—Sound Level Meters—Part 1: Specifications. International Electrotechnical Commission (IEC).

[39] Välimäki, V. and Reiss, J. (2016) All about Audio Equalization: Solutions and Frontiers. *Applied Sciences*, **6**, Article 129. https://doi.org/10.3390/app6050129

[40] Mahdjoub-Assaad, S. (2018) Nuisances Related to Road Traffic (Noise, Air Pollution and Insecurity): From Annoyance to the Perception of Health Risk from the Perspective of Social Inequalities. Ph.D. Thesis, University of Lyon, Lyon, France, 310 p.

[41] Dharmendra Kumar, K.V. and Srinivas, N. (2014) Study of Noise Levels in Very High Traffic Density Areas of Urban City. *International Journal of Engineering Research & Technology*, **3**, 1856-1861.

[42] Brown, A. and Van Kamp, I. (2017) WHO Environmental Noise Guidelines for the European Region: A Systematic Review of Transport Noise Interventions and Their Impacts on Health. *International Journal of Environmental Research and Public Health*, **14**, Article 873. https://doi.org/10.3390/ijerph14080873

[43] Ravinder, L. and Belachew, M.G. (2014) Urban Noise in a Metropolitan Towns. *Open Journal of Acoustics*, **4**, 163-176. https://doi.org/10.4236/oja.2014.44017

[44] Kardous, C.A., Shaw, P.B. and Murphy, W.J. (2016) Evaluation of Smartphone Sound Measurement Applications Using External Microphones—A Follow-Up Study. *Journal of the Acoustical Society of America*, **139**, 2036-2036. https://doi.org/10.1121/1.4950017

[45] Doyon-D'Amour, F., *et al*. (2024) Vibration Sensitivity of One-Port and Two-Port MEMS Microphones. arXiv: 2403.13643.

[46] Kardous, C.A. and Shaw, P.B. (2014) Evaluation of Smartphone Sound Measurement Applications. *The Journal of the Acoustical Society of America*, **135**, EL186-EL192. https://doi.org/10.1121/1.4865269

[47] STMicroelectronics (2014) Tutorial for MEMS Microphones. Application Note AN4426, DocID025704 Rev 1, 18 p.

[48] Serpanos, Y.C., Renne, B., Schoepflin, J.R. and Davis, D. (2018) The Accuracy of Smartphone Sound Level Meter Applications with and without Calibration. *American Journal of Speech-Language Pathology*, **27**, 1319-1328. https://doi.org/10.1044/2018_ajslp-17-0171

[49] Swain, B.K. and Goswami, S. (2014) Analysis and Appraisal of Urban Road Traffic Noise of the City of Cuttack, India. *Pakistan Journal of Scientific & Industrial Research Series A*: *Physical Sciences*, **57**, 10-19. https://doi.org/10.52763/pjsir.phys.sci.57.1.2014.10.19

[50] Halim, H. and Abdullah, R. (2014) Equivalent Noise Level Response to Number of Vehicles: A Comparison between a High Traffic Flow and Low Traffic Flow Highway in Klang Valley, Malaysia. *Frontiers in Environmental Science*, **2**, Article 13.

[51] Vijay, R., Kori, C., Kumar, M., Chakrabarti, T. and Gupta, R. (2014) Assessment of Traffic Noise on Highway Passing from Urban Agglomeration. *Fluctuation and Noise Letters*, **13**, Article ID: 1450031. https://doi.org/10.1142/s021947751450031x

[52] Serway, R.A. and Jewett, J.W. (2018) Physics for Scientists and Engineers with Modern Physics. 10th Edition, Cengage Learning.

[53] Baloye, D. and Palamuleni, L. (2015) A Comparative Land Use-Based Analysis of Noise Pollution Levels in Selected Urban Centers of Nigeria. *International Journal of Environmental Research and Public Health*, **12**, 12225-12246. https://doi.org/10.3390/ijerph121012225

[54] Sackey, L.N.A., Amuah, E.E.Y., Asamoah, D.K.O., Amoah, B., Amoyaw, B.C. and Tettey, B.A. (2025) Urban Noise Pollution in Kumasi Metropolitan Assembly, Ghana: Implications for Public Health and Quality of Life. *The Scientific World Journal*, **2025**, Article ID: 5769240. https://doi.org/10.1155/tswj/5769240

[55] Young, H.D. and Freedman, R.A. (2020) University Physics with Modern Physics. 15th Edition, Pearson.

[56] Urone, P.P. and Hinrichs, R. (2020) College Physics 2e. OpenStax, Rice University.

[57] Sombo, T., Nyitar, T., Tikyaa, E. and Igbawua, T. (2025) Investigation of Diurnal Road Traffic Noise in Makurdi Metropolis, Benue State, Nigeria. *African Scientific Reports*, **4**, Article 279. https://doi.org/10.46481/asr.2025.4.2.279

[58] Doygun, H. and Kuşat Gurun, D. (2007) Analysing and Mapping Spatial and Temporal Dynamics of Urban Traffic Noise Pollution: A Case Study in Kahramanmaraş, Türkiye. *Environmental Monitoring and Assessment*, **142**, 65-72. https://doi.org/10.1007/s10661-007-9908-7

[59] Tikyaa, E.V., Nyitar, T., Sombo, T. and Igbawua, T. (2025) Measurement and Mod-

elling of Diurnal Road Traffic Noise within Makurdi Metropolis, Benue State, Nigeria. *UMYU Scientifica*, **4**, 234-248. https://doi.org/10.56919/usci.2542.024

[60] Nyitar, T., Tikyaa, E.V., Sombo, T. and Igbawua, T. (2025) Analysing the Relationship between Diurnal Road Traffic Noise and Meteorological Variables in Makurdi Metropolis, Nigeria. *Fudma Journal of Sciences*, **9**, 228-240. https://doi.org/10.33003/fjs-2025-0906-3726

[61] Olayinka, O.S. and Oloyede, O.O. (2014) Assessment of Traffic Noise Pollution in Selected Urban Areas of Nigeria. *Environmental Monitoring and Assessment*, **186**, 7895-7907.

[62] Nath, H., Adhikary, S.K., Alsulamy, S., Kafy, A.A., Rahaman, Z.A., Roy, S., *et al*. (2024) Assessment of Index-Based Traffic Noise Annoyance Level at Major Road Intersections in a Tourist City: A Case Study towards Environmental Sustainability. *Heliyon*, **10**, e40005. https://doi.org/10.1016/j.heliyon.2024.e40005

[63] Olayinka, O.S. (2009) Assessment of Noise Pollution Levels in Selected Areas of Ilorin Metropolis, Nigeria. *Environmental Monitoring and Assessment*, **158**, 155-167.

[64] Singh, N. and Davar, S.C. (2004) Noise Pollution-Sources, Effects and Control. *Journal of Human Ecology*, **16**, 181-187. https://doi.org/10.1080/09709274.2004.11905735

[65] Clark, S.N., Arku, R.E., Ezzati, M., Bennett, J., Nathvani, R., Alli, A.S., *et al*. (2025) Moving beyond the Noise: Geospatial Modelling of Urban Sound Environments in a Sub-Saharan African City. *Scientific Reports*, **15**, Article No. 21403. https://doi.org/10.1038/s41598-025-06537-1